JETIR.ORG ISSN: 2349-5162 | ESTD Year : 2014 | Monthly Issue
JOURNAL OF EMERGING TECHNOLOGIES AND INNOVATIVE RESEARCH (JETIR)
An International Scholarly Open Access, Peer-reviewed, Refereed Journal

Detection of Cell Nuclei In Cervical Cytology ImagesUsing U-Net And Res-Net Neural Networks

Parth Gaikwad [1], Aditya Patil [2], Shubham Nalawade [3], Ms. K. P. Joshi[4]

E&TC Dept., SKNCOE , SPPU , Pune

parthgaikwad752@gmail.com

adityapatil241998@gmail.com

nalawade.Shubham123@gmail.com

Abstract— **The effective adoption of the U-Net and ResNet50 is used to identify nuclei. The majority of the related researches have relied on conventional computer vision techniques such as morphological image analysis, data mining, and so on, however the strategy identified in this survey paper uses machine learning techniques to improve accuracy. The ResNet and U-Net is used to efficiently conduct nuclei detection on a dataset of cervical cytology pictures. The provided method derives these qualities from a precise implementation that has resulted in the realization of the training of these neural networks. These models are trained on cervical cytology images dataset that is provided as an input. The trained models are then used for deployment of the test cervical cytology images to determine the performance of these models. The experimental evaluation of the approach has been performed which has resulted in highly accurate results portrayed in this research article.**

Keywords— **U-net, Res-Net, Image Processing, Cervical Cell and Cell nuclei.**

I. Introduction

Cancer refers to a category of disorders in which the body's cells grow, alter, and replicate uncontrollably. Cervical cancer is defined as the uncontrollable proliferation of cells that start in the cervix's tissues. It is one of the largest prevalent gynecological cancers, with a cure rate of virtually 100 percent when diagnosed and managed early. The Pap smear is a screening procedure that involves depositing a specimen of tissue from the uterine tract upon a glass slide for direct inspection in order to determine pre-cancerous abnormalities. It is extensively employed in advanced nations, and it has greatly reduced the frequency of the disease and the proportion of fatalities associated with it.

Conversely, in undeveloped nations, demographically scanning is still totally inaccessible, owing to the difficulty and time-consuming aspect of individually evaluating anomalous cells from cervical cytology samples. Although automated enhanced scanning approaches can increase productivity, their present performance is insufficient for baseline cervical assessment. In past few years, there seems to be an upsurge in the number of women diagnosed with cervical cancer. Cervical cancer is among the most severe kinds of cancer that may be excruciatingly painful and devastating if not identified early. Doctors advocate regular Pap screening testing or cytology tests to make a diagnosis before it becomes lethal for women in order to lower mortality rates.

Cervical cancer is easily treatable and could provide respite from death and discomfort. As a result, the most important requirements for reducing cervical cancer growth are competent and prompt detection. Through use of a Cancer screening or cytology of the cervix is used to identify and diagnose cervical cancer. The Pap smear examination examines the tissues of the cervix to see whether any malignant or premalignant cells can be found. Just about all females require this sort of test on a frequent basis since it enables for careful detection and monitoring of cervical cancer. The Pap smear is transferred to a slide and viewed individually by a healthcare professional, who describes the cells found.

The samples are viewed under a microscope, each one of the cells is thoroughly scrutinised by the specialist to discover malignant and premalignant cells. The quantity of cells and images is large, and the procedure is patiently carried out by the physician. This form of categorization needs patience, and because it is done by hand, there is a considerable possibility of human error creeping into the assessment. Because the manual inspection is conducted by a medical expert, it consumes a significant amount of the doctor's time, which may be better spent on other vital activities. This seems to be an unfavorable situation that can be exceedingly harmful to the patient who is being evaluated. As a result, a reliable and automated classification scheme for cervical cancer cytology is required.

To design an efficient and precise approach for the categorization of cervical cells, a number of obstacles must always be resolved. The cells in the cervical cytology images must always be investigated separately in depth. This is very simple for a

person to accomplish, but it becomes progressively harder for an individual to accomplish. As a result, the image processing framework based on machine learning offers a feasible answer to this large problem. The nuclei of the cervical cells are used to identify the cells. This enables the algorithm to identify the cells and examine them more closely.

The Literature Survey component of this research paper examines previous work. Section 3 delves into the approach in depth, while section 4 focuses on the outcomes evaluation. Finally, Section 5 brings this report to a close and gives some hints for future research.

II. Literature Survey

H. Chang et al. [1] developed and implemented a multireference thresholding approach for detecting nuclei from H&E-stained tumour slices to the TCGA GBM cohort. They are able to enhance the efficiency of biological and technical variations by merging relevant data from manually labeled reference photographs with local information from the target image'sdeconstructed nuclear channel. The experimental outcomes and comparisons illustrate the efficacy of the suggested strategy.

A revolutionary smartphone-based cloud-assisted approach for leukocyte categorization and segmentation in blood smear pictures has been presented by M. Sajjad et al., which would aid haematologists in identifying different illnesses more quickly and accurately. To this purpose, the proposed technology enables medical professionals to monitor and make prompt judgments concerning anomalous discoveries in the target population in smart cities by providing individuals with convenient access to high-quality healthcare services at any time and from any location [2]. Instead of sending an entire diagnostic image dataset, offload image features to the cloud to train a multi-class classifier and save internet bandwidth. A colour K-means clustering technique is implemented into the proposed framework for efficient and effective segmentation, yielding superior segmentation results than previous state-of-the-art systems.

K. S. Beevi et al. presents a methodology for segmenting and classifying mitotic nuclei in breast histopathology pictures that is both effective and accurate. Mitosis is difficult to distinguish from non-mitotic nuclei since it is uncommon and well separated. To simplify the process of segmenting accurate nuclei boundaries in big clinical pictures, the suggested approach initially uses a stain normalization process. The KHA-based LACM solves the problem of segmenting accurate nuclei boundaries in the most efficient way possible [3]. To recognize mitotic candidates from the contour segmented nuclei areas, a multi classifier depend on deep belief networks is used. Individual classifier outputs are also improved by sequential feature selection and feature normalization. By adjusting the weights of individual classifiers throughout the training phase, the DBN-MCS greatly enhances the sensitivity score when compared to majority voting-based MCS. The suggested method is tested on a publicly available standard dataset as well as clinical data from a leading cancer research facility.

Z. Zeng et al. propose a redesigned network architecture that uses RI and DC blocks to help the network learn more effective features and produce more accurate nucleus segmentation results [4]. This network may be superior to previous approaches not only in terms of analyzing indicators, but also in terms of cost-effectiveness, allowing clinicians to better diagnose the subtleties of these histological pictures. To overcome the problem of various cell forms, the proposed model was exposed to greater extraction of global and local context to enable it to detect different types of cell shapes and cells of different sizes. Meanwhile, to cope with the problem of dense cell overlap, the authors used the multi-task learning framework in the segmentation of gland instances, allowing the network to train to segment the nucleus and cell contour at the same time. The cell contour will be used as supplementary information to aid in the differentiation of dense cells and eliminate mistakes at the object level by this network.

L. Feng et al. [5] describe a basic module that learns from a few sample annotations and then detects unlabeled nuclei. This module is part of the Mask R-CNN framework, and it shows how the suggested approach can consistently train from a partially labelled dataset. As a consequence, the presented strategy takes fewer training datasets than its predecessor and produces comparable results to the baseline method, reducing the time necessary to prepare training datasets. While training with partial annotations, detection performance is somewhat degraded since the presented network has less samples from which to learn.

F. Li et al. suggest a contour detection model depend on the information response process seen in biological visual systems. An image's colour information and grayscale information are processed selectively. Some retinal/LGN neurons reflect colour information's single-opponent properties, while others reflect grayscale information's linear and nonlinear response characteristics. The directional neurons in the V1 visual cortex reflect the colour information's double-opponent properties as well as the grayscale information's excitatory–inhibitory (center–surround) properties [6]. By introducing a parallel information response unit (a colour channel response based on image colour information and a luminance channel response based on image grayscale information), the combined weights of the colour channel response and the luminance channel response are calculated to obtain the final contour response, based on the dual features of colour and grayscale, thus combining the optimal direction of each pixel and the complementary nature of the image in the final contour response.

The appearance of the cervical nucleus is critical for distinguishing between normal and dysfunctional cervical cells. Because the findings of nuclear edges prediction and nuclear boxes prediction are not employed in the classification branch of Mask R-CNN, the original RoI features are scaled from variable sizes to fixed sizes. B. Ma et al. suggested FPM keeps the size of the cervical nucleus the same, allowing to extract and detect the characteristics of aberrant cervical cells more efficiently [7]. Additionally, the attention method is utlized to blend the original RoI features with the predefined length of RoI features, leading to enhanced classification discriminations. The convolution layer can improve the classification accuracy of the networkmodel even further. Experiments outcome that the MACD R-CNN technique greatly outperforms the Mask R-CNN method.

M. Valkonen et al. explored how histopathological sample fixation affected the accuracy of a nuclei identification algorithm trained on hematoxylin and eosin-stained pictures [8]. The supervised transfer learning was utilized to train a convolutional neural

network baseline model for nuclei detection. The authors used unsupervised domain adaptation as the second part of the algorithm to allow generalisation to photos from previously unexplored domains, such as other tissues and images from various laboratories, without the necessity for labelled data. The main contributions are to explore the effect of sample fixation on nuclei detection accuracy using hematoxylin and eosin-stained training images prepared with three fixation methods: PAXgene, formalin, and frozen, and to provide the presented extensive multi-fixation dataset with manually obtained annotations for cell locations, which will aid in method development.

To enhance nuclei detection in huge 3D fluorescence datasets, M. Lapierre-Landry et al. introduce VRegNet, a unique mix of nuclei-segmentation and centroid-regression networks. Even though the tissue types comprised clustered nuclei of various forms, sizes, and fluorescent intensity, this innovative technique was able to detect centroids with excellent accuracy in both intact quail embryonic hearts and the mouse brain stem [9]. When tested on a cardiac sample that was not included in the training dataset, VRegNet was resilient and maintained equal accuracy, and it rapidly adapted to the brain stem pictures with minimum fine-tuning. The VRegNet also preserved the nuclei's spatial distribution in the manually segmented ground-truth data.

J. Huang et al. propose a new approach for segmenting cervical cells depend on the Cell-GAN. By measuring the integrity of a cell using the probability distribution of cell morphology, the Cell-GAN provides a single-cell picture for each cell to be segmented in the cell image. The shape of the produced cell serves as the final segmentation line. Segmentation success is ensured by the guide factor used to identify the cell in the segmentation process, especially for overlapping cells. R-crop, an automated image cropping technique, improves segmentation performance even further [10]. By calculating probability distributions and comprehending the common properties of cervical cells, the proposed approach efficiently overcomes cell overlapping issues. The segmentation results reveal that the proposed Cell-GAN technique may accomplish comprehensive segmentation capacity, particularly in the situation of highly overlapping cells and complicated backdrops, with a much lower segmentation failure rate than the other four methods.

For cell nuclei in colon cancer histopathology pictures, a phased detection–identification paradigm was presented by X. Li et al. A POI detector and an MC-Net classifier were included in the suggested technique. The POI model was created to increase the sensitivity of identifying nuclei by integrating cascade blocks for decoding the complementary information of multiple level characteristics. The MC-Net classifier, on the other hand, was created to give perfectibility of information by including a multicropping module for gathering contextual contents at multiple areas for nuclei [11]. The suggested detection–identification framework might take advantage of the knowledge of numerous aspects to achieve improved performance, according to experimental results using public histopathology data.

F. Xing et. al. [12] presents a new FCN architecture for single-stage nucleus recognition that can be trained efficiently end-to-end, pixel-by-pixel. The authors characterize nucleus recognition as a structured regression problem that may take use of contextual information in the label space, rather than pixel-wise classification. The suggested method, in contrast to many earlier nucleus/cell recognition systems, which often rely on a multi-stage image processing pipeline, allows for single-stage, simultaneous nucleus detection and classification. Meanwhile, because nucleus segmentation is difficult, especially for a single picture with hundreds of nuclei, it does not require each nucleus segmentation for cellular feature extraction, which may considerably enhance the efficiency and efficacy of image quantification.

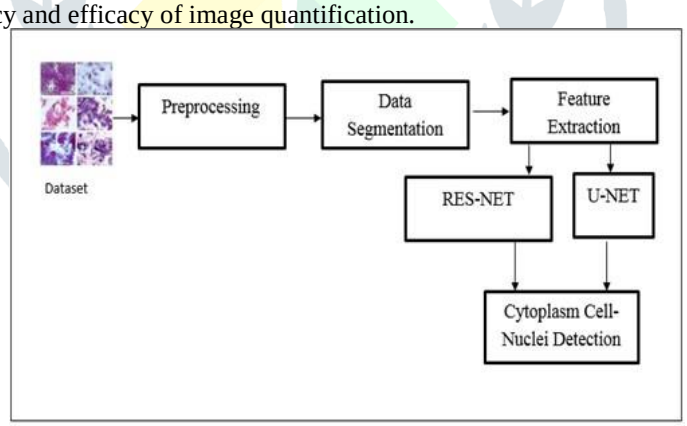

III PROPOSED METHODOLOGY

Figure 1: Proposed model for Cytoplasm Nuclei Detection

Step 1: Pre-processing and Data Segmentation: The developed project for nuclei detection in cytology images is deployed using the Dataset from the URL: https://github.com/parham-ap/cytology_dataset. This dataset contains 93 cytology images and their respective EDF (Extended depth of field) images acquired from three grades like negative, LSIL and HSIL.

Step 2: Feature Extraction - The original cytology images of the dataset and corresponding mask images are fed to the system for the purpose of nuclei detection process. Here in this process out of 93 dataset cytology images 73 are separated as training images and remaining 20 images are used for the testing purpose. The process of implementing UNET and RES net models are explained in the following sections thoroughly.

Step 3: UNET- The U-Net is implemented on the cervical cytology images to achieve detection of the cytoplasm. The U-Net achieves an effective identification of the cytoplasm by taking the input of train images and the respective mask images along with the test images and the respective mask images. The U-Net has been implemented through the realization of the characteristic of this architecture that performs expansion and then contraction. In between the contraction and the expansion process, is a traditional CNN that is implemented. For this purpose, there are 10 layers each for the expansion process and the contraction process.

The layers implemented for the expansion have the filter set at 16, with the activation function as relu and 3x3 kernel along with the kernel initializer as he normal through the keras approach. The dropout is utilized between the layers to prevent any problems with overfitting with the dropout rate set at 0.1. The max pooling operation is performed for a 2x2 of pooling window. The next two layers have the same initialization but with the filter set at 32. With identical dropout in-between the layers and similar pooling operations. The next two layers have the filters increased to 64 and the change of the dropout rate to 0.2, the pooling though remains the same.

The consecutive two layers have the filter set at 128 with the dropout rate still at 0.2. The filter is further increased in the two expansion to 256 and the dropout rate at 0.3. The pooling is not implemented here, rather the conv2Dtranspose is used, which is also referred to as the deconvolution operation. This operation learns the best upsampling that can be implemented intothe model. Here, a conv2Dtranspose is realized using 128 as the filter, kernel size of 2x2 and the stride set at 2x2. The layers arethen concatenated effectively.

The contraction procedure involves the reduction of the filters consistently from 128 to 64 and concatenation with the respective expansion layer in addition to a conv2Dtranspose with the filter set at 64. The dropout rate is reduced to 0.1 when the filter is set at 32 and the conv2Dtranspose is used with the similar structure as before but with a reduced filter set at 32. This is repeated further with the decreasing values of filter sizes for the conv2D at 32 and the Conv2Dtranspose at 16. The last set of layers utilize the filter size at 16 and an output layer with filter at 1 ,kernel size at 1x1 and the sigmoid activation function. The loss is optimized by adam optimizer.

Step 4: RES-NET: The ResNet50 approach is implemented to achieve the effective result through the realization of all of the components of the approach. The code snippet depicting the ResNet50 is depicted in the figure g given below. Firstly, the images are provided to the approach and the zero padding is added with the padding of 3x3. After this step the first stage of the approach is realized where a conv2D layer with filter set at 64, kernel size of 7x7, strides of 2x2, and the glorot uniform kernel initializer with seed set at 0. The batch normalization has been realized using the channel axis of the input set at 3 and the relu activation function. The pooling has been done through maxpooling2D with pool size window of 3x3 and strides at 2x2.

The second stage involves the implementation of a Convolution block that implements a set of filter of size 64, 64, 256, with f at 3, s as 1 and block is set as a. In the second state there are two identify blocks that are used, these identity blocks use filters of the size 64, 64, 256, with f as 3 with blocks c and b. The third stage utilizes a convolution block with the size of filters being 128, 128, 512 with s being set as 2, f as 3 and the block as a. In this stage there are three identity blocks, with filters at 128, 128, 512, with blocks c, b and d, along with f set as 3.

The stage 4 realizes a convolutional block with filters set as 256, 256 and 1024 with the block being a and s as 2 and f as 3. The identity blocks in this stage are 5 in number with filters at 256, 256, 1024 with blocks as e, f, b, c, d, and f as 3. The stage 5 uses a convolution block with 512, 512, 2048 with blocks c and b and f as 3. There are two identity blocks that are used with blocks c and b, with f as 3 and filter size as 512, 512, 2048.

An average pool is implemented with the shape of the window as 2, 2 for the average2D pooling. The flatten is realized as an output layer and an input reduction is attained as a dense fully connected layer which uses the sigmoid activation function and a glorot uniform kernel initializer of seed as 2.

Step 5: Nuclei and Cell marking - The process of nuclei identification is performed on the obtained resulted individual cytology image collected in the list. The individual cytology image is scanned in two ways, left to right and top to bottom. This process performed iteratively to assess each pixel and its value to determine the cytoplasm boundary. Once the boundary is encountered, the algorithm stops at the boundary and marks an area 15 pixels from the left and top into the cytoplasm as the location of the nucleus. The detected all the nuclei positions are stored in a list which is then processed further for the marking and result evaluation process.

IV. RESULTS AND DISCUSSIONS

The proposed methodology for nuclei detection in cervical cytology images has been outlined in this article. To achieve the prescribed goals a development machine with a standard configuration has been used. The development machine is powered by an Intel i5 processor equipped with 6 GB of RAM. The python programming language was used to achieve the proposed model. The presented technique has been developed using the python programming language through the Spyder IDE. For achieving effective image processing, the Keras and TensorFlow libraries are utilized.

The Keras library is a high-level Python library that is used as a wrapper for low-level libraries. The Keras library contains the neural networks that can be interfaced with low-level libraries such as TensorFlow. TensorFlow is an open-source library designed by Google that allows the application of deep learning techniques.

For the extraction of the performance metrics of the algorithms utilized in this approach the paradigm of precision, recall, and F-Measure is implemented. The precision is the ratio of correctly identified nuclei to the total number of correct identifications. The Recall is the ratio of correctly identified nuclei to the total number of identifications. Thus, the F-measure achieves the balance between precision and recall as a weighted measure as a harmonic mean of both precision and recall. The equations for the calculation of these performance metrics are provided in equations 1, 2, and 3 below.

$$Precision = \frac{TP}{TP+FP} \text{ ---------- (1)}$$

$$Recall = \frac{TP}{TP+FN} \text{ ---------- (2)}$$

$$F - Measure = \frac{2*Precision*Recall}{Precision+Recall} \text{ --- (3)}$$

Where,

TP= True Positives
FN= False Negatives
FP= False Positives

In our evaluation approach, the values of True Negative (TN) is zero. The obtained results from our experiment are depicted in the following table 1 and 2 for, UNet, and ResNet50 respectively.

Testing Image No	True Positve	False Positive	False Negative	UNet Precision	UNet Recall
73	29	2	1	0.935483871	0.96667
74	15	2	0	0.882352941	1
75	48	9	8	0.842105263	0.85714
76	20	2	2	0.909090909	0.90909
77	6	1	0	0.857142857	1
78	22	3	2	0.88	0.91667
79	14	1	0	0.933333333	1
80	15	1	0	0.9375	1
81	10	1	0	0.909090909	1
82	11	1	0	0.916666667	1
83	6	1	0	0.857142857	1
84	6	1	0	0.857142857	1
85	3	1	0	0.75	1
86	6	2	0	0.75	1
87	10	2	1	0.833333333	0.90909
88	19	1	0	0.95	1
89	10	1	0	0.909090909	1
90	21	3	2	0.875	0.91304
91	21	1	0	0.954545455	1
92	19	2	0	0.904761905	1

Table 1: UNET Results

Testing Image No	True Positve	False Positive	False Negative	ResNet50 Precision	ResNet50 Recall
73	30	1	1	0.967742	0.967742
74	15	2	0	0.882353	1
75	49	8	8	0.859649	0.859649
76	20	2	2	0.909091	0.909091
77	6	1	0	0.857143	1
78	22	3	2	0.88	0.916667
79	14	1	0	0.933333	1
80	15	1	0	0.9375	1
81	10	1	0	0.909091	1
82	11	1	0	0.916667	1
83	6	1	0	0.857143	1
84	6	1	0	0.857143	1
85	3	1	0	0.75	1
86	6	2	0	0.75	1
87	10	2	1	0.833333	0.909091
88	19	1	0	0.95	1
89	10	1	0	0.909091	1
90	21	3	2	0.875	0.913043
91	21	1	0	0.954545	1
92	19	2	0	0.904762	1

Table 2: RES-NET Results

The results obtained through the Precision, Recall, and F-Measure procedures are tabulated and compared in table 3 given below. The values are represented graphically in figure 2.

Methodology	Precision ± STD	Recall ± STD	F-Measure
U-Net	0.8821 ± 0.0576	0.9735 ± 0.0450	0.9256
ResNet50	0.8846 ± 0.0590	0.9737 ± 0.0447	0.927

Table 3: U-Net and ResNet50 comparisons.

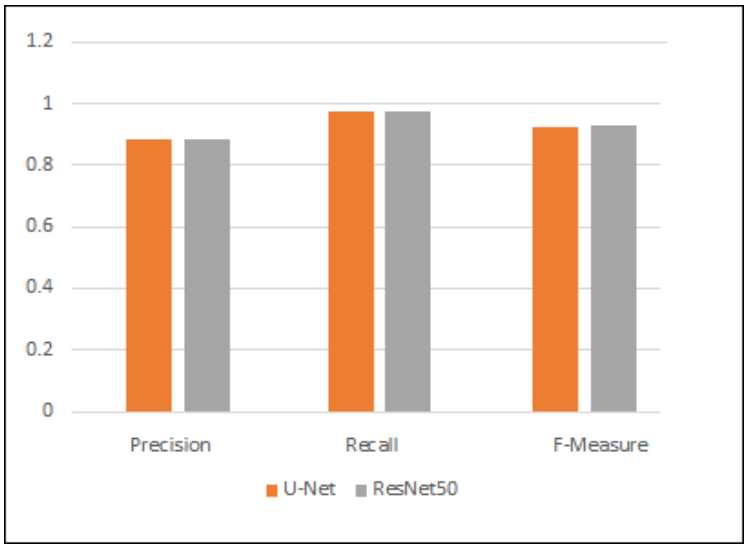

Figure 2: Graphical representation of the comparison.

The results indicate that the ResNet50 and U-Net approaches are highly effective for the detection of nuclei accurately.

V CONCLUSION AND FUTURE SCOPE

The proposed methodology to enable effective and accurate cell nuclei detection in cervical cytology images has been outlined in this research article. The paradigm of cervical cytology is essential as it is one of the most effective ways of detecting cervical cancer. This methodology concentrates on the paradigm of cervical cytology nuclei detection through the use of machine learning approaches such as U-Net, ResNet50, and CNN which are combined in an ensemble technique.

The nuclei in the cervical cytology are detected using the 2 neural networks and an ensemble approach is highlighted effectively. The paradigm of Precision and recall performance metrics is utilized to achieve the performance of the approach. The results of the precision and recall are achieved for each of the algorithms and are detailed effectively. The precision achieved by the proposed methodology is 88.46 which is an exceptional result. The methodology has been compared with the conventional technique for cervical cytology nuclei detection and has come to the conclusion that the presented technique significantly outperforms. The improvement is considerable as it proves the superiority of the ensemble technique outlined in this research article.

In the future, the methodology can be implemented in a real-time scenario. The approach can be effectively utilized to process and identify the nuclei in cervical cell cytology to achieve effective and fast identification. The approach can also be improved further to increase the accuracy to 100% that can be highly beneficial in improving the cervical cytology cell nuclei detection approach that can save countless lives with great efficiency and reliability.

ACKNOWLEDGMENT

It gives us great pleasure and satisfaction in presenting this project report on “Cell Nuclei Detection in Cervical Cytology Images Using Res-Net And U-Net Neural Networks ”. We thankful to and fortunate enough to get constant encouragement, support and guidance from all Teaching staffs of [E & TC Dept] which helped us in successfully completing our project work. Also, We would like to extend our sincere esteems to all staff in laboratory for their timely support.

REFERENCES

[1] H. Chang, J. Han, P. T. Spellman and B. Parvin, "Multireference Level Set for the Characterization of Nuclear Morphology in Glioblastoma Multiforme," in IEEE Transactions on Biomedical Engineering, vol. 59, no. 12, pp. 3460-3467, Dec. 2012, doi: 10.1109/TBME.2012.2218107.

[2] M. Sajjad et al., "Leukocytes Classification and Segmentation in Microscopic Blood Smear: A Resource-Aware Healthcare Service in Smart Cities," in IEEE Access, vol. 5, pp. 3475-3489, 2017, DOI: 10.1109/ACCESS.2016.2636218.

[3] K. S. Beevi, M. S. Nair and G. R. Bindu, "A Multi-Classifier System for Automatic Mitosis Detection in Breast Histopathology Images Using Deep Belief Networks," in IEEE Journal of Translational Engineering in Health and Medicine, vol. 5, pp. 1-11, 2017, Art no. 4300211, DOI: 10.1109/JTEHM.2017.2694004.

[4] Z. Zeng, W. Xie, Y. Zhang and Y. Lu, "RIC-Unet: An Improved Neural Network Based on Unet for Nuclei Segmentation in Histology Images," in IEEE Access, vol. 7, pp. 21420-21428, 2019, DOI: 10.1109/ACCESS.2019.2896920.

Exemplars," in IEEE Access, vol. 7, pp. 162169-162178, 2019, DOI: 10.1109/ACCESS.2019.2952098.

[6] F. Li, C. Lin, Q. Zhang and R. Wang, "A Biologically Inspired Contour Detection Model Based on Multiple Visual Channels and Multi-Hierarchical Visual Information," in IEEE Access, vol. 8, pp. 15410-15422, 2020, DOI: 10.1109/ACCESS.2020.2966916.

[7] B. Ma, J. Zhang, F. Cao and Y. He, "MACD R-CNN: An Abnormal Cell Nucleus Detection Method," in IEEE Access, vol. 8, pp. 166658-166669, 2020, DOI: 10.1109/ACCESS.2020.3020123.

[8] M. Valkonen, G. Högnäs, G. S. Bova and P. Ruusuvuori, "Generalized Fixation Invariant Nuclei Detection Through Domain Adaptation Based Deep Learning," in IEEE Journal of Biomedical and Health Informatics, vol. 25, no. 5, pp. 1747-1757, May 2021, DOI: 10.1109/JBHI.2020.3039414.

[9] M. Lapierre-Landry, Z. Liu, S. Ling, M. Bayat, D. L. Wilson and M. W. Jenkins, "Nuclei Detection for 3D Microscopy With a Fully Convolutional Regression Network," in IEEE Access, vol. 9, pp. 60396-60408, 2021, DOI: 10.1109/ACCESS.2021.3073894.

[10] J. Huang, G. Yang, B. Li, Y. He and Y. Liang, "Segmentation of Cervical Cell Images Based on Generative Adversarial Networks," in IEEE Access, vol. 9, pp. 115415-115428, 2021, DOI: 10.1109/ACCESS.2021.3104609.

[11] X. Li, W. Li and R. Tao, "Staged Detection–Identification Framework for Cell Nuclei in Histopathology Images," in IEEE Transactions on Instrumentation and Measurement, vol. 69, no. 1, pp. 183-193, Jan. 2020, DOI: 10.1109/TIM.2019.2894044.

[12] F. Xing, T. C. Cornish, T. Bennett, D. Ghosh and L. Yang, "Pixel-to-Pixel Learning With Weak Supervision for Single-Stage Nucleus Recognition in Ki67 Images," in IEEE Transactions on Biomedical Engineering, vol. 66, no. 11, pp. 3088-3097, Nov. 2019, DOI: 10.1109/TBME.2019.2900378.